Electrochimica Acta 341 (2020) 136022

Contents lists available at ScienceDirect

Electrochimica Acta

journal homepage: www.elsevier.com/locate/electacta

Selective electrochemical hydrogen evolution on cerium oxide protected catalyst surfaces

Balázs Endrődi [a, *], Oscar Diaz-Morales [b], Ulriika Mattinen [b], Maria Cuartero [c], Aiswarya Krishnakumar Padinjarethil [d], Nina Simic [e], Mats Wildlock [e], Gaston A. Crespo [c], Ann Cornell [b, **]

[a] Department of Physical Chemistry and Materials Science, University of Szeged, Rerrich B. Square 1., H-6720, Szeged, Hungary
[b] Applied Electrochemistry Division, School of Engineering Sciences in Chemistry, Biotechnology and Health, KTH Royal Institute of Technology, Teknikringen 42, SE 100-44, Stockholm, Sweden
[c] Applied Physical Chemistry Division, School of Engineering Science in Chemistry, Biochemistry and Health, KTH Royal Institute of Technology, Teknikringen 30, SE-10044, Stockholm, Sweden
[d] Department of Energy Conversion and Storage, Technical University of Denmark, Fysikvej, 2800, Kgs. Lyngby, Denmark
[e] Nouryon Pulp and Performance Chemicals AB, Färjevägen 1, SE 445-80, Bohus, Sweden

ARTICLE INFO

Article history:
Received 9 January 2020
Received in revised form
4 March 2020
Accepted 4 March 2020
Available online 6 March 2020

Keywords:
Cathode selectivity
HER
Industrial electrochemistry
Chemical technology
Dichromate

ABSTRACT

To date the only known solution to avoid the unwanted electrochemical reduction of hypochlorite and chlorate in industrial chlorate production, performed in undivided cells, is the addition of dichromate to the chlorate electrolyte. Because of the toxicity of this compound its use is restricted within the European Union to time limited authorization by REACH. Therefore, an alternative to sodium dichromate is essential to maintain, or even increase the process efficiency.

The addition of cerium (III) salts to a hypochlorite solution increases the cathodic selectivity towards hydrogen evolution (HER), the preferred cathode process in industrial chlorate production. This is attributed to the deposition of a thin cerium oxide/hydroxide coating on the cathode, induced by the increased local alkalinity during electrolysis.

Performing the electrodeposition of such protective coating ex situ, well-controlled coating thickness can be achieved. Optimizing the deposition conditions (time, current density), a coherent and stable coating is formed on the electrode surface. On this protected electrode surface the electrochemical reduction of hypochlorite is suppressed by ca. 90% compared to the bare Pt electrode, while the HER proceeds with high selectivity and unchanged kinetics. Interestingly, other electrochemical reactions (O_2 reduction, H_2O_2 reduction and oxidation) are also suppressed by the protective coating, suggesting that the deposited layer acts as an inorganic membrane on the electrode surface.

1. Introduction

Selectivity of the electrode reactions is an essential question for all the processes involving electrochemical techniques. Unwanted side reactions decrease the Faradaic efficiency of the desired process in hand, hence increasing the production cost. These could also lead to the formation of harmful products, thus poisoning the electrocatalysts or damaging the cell structure (e.g. corrosion). The electrode selectivity is crucial both in industrial processes, e.g. chlor-alkali or chlorate electrolysis[1], and in more fundamental applications, e.g. photo (electro)catalytic water splitting or CO_2 electrolysis [2].

Fundamental science and mature electrochemical industries therefore share a joint need for selective electrode processes. For example, in commercial chlorate production in undivided electrolytic cells, the reduction of chlorate and hypochlorite is hindered in favour of hydrogen evolution by addition of sodium dichromate. Another widely applied solution to avoid the reduction of anodic products on the cathode, and oxidation of the cathodic products on the anode is to design cells in which the cathode and anode chambers are separated by a membrane or diaphragm, as in

* Corresponding author.
** Corresponding author.
E-mail addresses: endrodib@chem.u-szeged.hu (B. Endrődi), amco@kth.se (A. Cornell).

https://doi.org/10.1016/j.electacta.2020.136022

polymer electrolyte membrane (PEM) water electrolysis[3] or the chlor-alkali synthesis [4]. However, the re-design of a mature chlorate process requires a more or less new plant design as well, due to the large difference in process design between a membrane process and a single compartment process, entailing huge investment costs [5]. In addition, there are several challenging issues with using a membrane cell in chlorate production e.g. presence of chlorate in anolyte leading to ClO_2 formation posing a safety risk and efficiency loss and the inherent unfavourable water balance, lowering energy efficiency. In other related cases, such as in photochemical water splitting the reaction between the formed H_2 and O_2 must be circumvented. This reaction normally proceeds rapidly on the co-catalyst surface [6]. As H_2 and O_2 forms on the same catalyst particle, they cannot be separated by a membrane placed between the catalyst particles, the co-catalyst itself has to be "protected".

Coating the electrode surface with different amorphous oxide films were proved to increase the electrode selectivity towards hydrogen evolution reaction (HER) or decrease the recombination of the products on the catalyst surface [7–11]. This latter effect is typically attributed to the semi-permeable, membrane-like nature of these coatings, allowing the transfer of water and the products through them, but not that of other reactants, such as dissolved oxygen. Analogously, amorphous oxide coated electrodes were proved to suppress the electrochemical reduction of sodium hypochlorite, an unwanted reaction during the electrolytic synthesis of sodium chlorate [12–15]. Note that in the latter case density functional theory (DFT) calculations showed that the active site for hypochlorite reduction becomes blocked in the course of its reduction on various catalytic surfaces, which can be another significant factor for the increased HER selectivity on these in hypochlorite solutions [16].

Sodium dichromate is added to the chlorate electrolyte in the currently applied industrial technology, which leads to the almost complete suppression of hypochlorite reduction [1]. This is caused by the deposition of a thin chromium oxide/hydroxide layer on the cathode surface [17]. In this case the deposition is self-terminated, leading to the formation of a thin layer on the electrode surface [18]. Further, as the sodium dichromate remains in the electrolyte the layer is re-formed during electrolysis in case of any damage or dissolution during operation shutdown, hence the layer is "self-healing". The use of sodium dichromate has long been considered as the optimal solution for the electrolytic synthesis of sodium chlorate. However, due to health and safety considerations the use of chromium (VI) compounds in industrial processes has been banned in the European Union unless a time limited Authorization is given. Similar regulations are expected in other parts of the World as well [1]. An alternative synthesis route, or the direct replacement for sodium dichromate is therefore highly demanded by the chlorate producers.

Rare earth metal (REM) salts[12], sodium molybdate [13], sodium permanganate [14] or sodium metavanadate[15] addition were shown to suppress the unwanted electroreduction of hypochlorite under specific circumstances. Nevertheless, under industrial conditions the low solubility of REM salts was found to be an obstacle, while sodium molybdate was not effective enough in this case. As for the permanganate additive, the continuous deposition of a manganese oxide layer led to the formation of too thick and mechanically unstable coatings, while vanadate addition led to the unwanted decomposition of hypochlorite to oxygen, which is both an efficiency loss and a safety issue in the process. Despite the results showing that these pathways are not realistic alternatives for the use of sodium dichromate, based on the reported results the requirements can be much clearly and critically addressed. To replace sodium dichromate directly in the sodium chlorate synthesis process a compound must be found that: (i) leads to high cathodic HER selectivity, (ii) does not decrease the anodic current efficiency for chlorine evolution, (iii) decreases the decomposition of hypochlorite to oxygen [19–21] (iv) preferably buffers the solution in the pH = 6.5–7 range and (v) leads to the formation of a thin and self-healing coating, which does not decrease the energy efficiency of the process (e.g. increased cell voltage). Evidently, the role of a potential replacement candidate is very demanding. Partly fulfilling these, the use of ex situ formed, selective cathodes is also a realistic option to maintain high process efficiency for electrochemical sodium chlorate production [22–24].

Sweeping through potential candidates, the stability of different electrode coatings under chlorate electrolysis conditions must be considered. During operational stops, the hot, close to neutral chlorate electrolyte is a very oxidative medium. During electrolysis, the electrode is polarized at negative potentials, which also leads to a local pH increase. An ideal electrode coating must withstand both these extremities. Judging simply upon thermodynamic considerations (e.g. Pourbaix diagrams)[25], cerium oxides/hydroxides might be ideal candidates.

In this study we present the effect of cerium (III) salt addition on the electrochemical reduction of hypochlorite, which is an important intermediate during the electrochemical synthesis of sodium chlorate. We herein demonstrate that this unwanted reduction reaction can be effectively suppressed this way, which is attributed to the deposition of a cerium oxide/hydroxide layer on the cathode. Further, to avoid the difficulties caused by the precipitation of cerium hydroxide in the electrolyte bulk, we evaluate cerium oxide coated cathodes, formed ex situ by electrodeposition, in the same reaction. We demonstrate, that the electrode selectivity is related to the deposited layer, and not to the presence of dissolved cerium (III) in the solution.

2. Experimental

2.1. Reagents and solutions

NaOCl (0.5 M solution in 0.1 M NaOH), H_2O_2, NaCl and $NaClO_4$ were purchased from VWR International, while $CeCl_3$ and $Ce(NO_3)_3$ hexahydrate was from Sigma-Aldrich. All chemicals were of analytical grade and were used as received. Commercially available buffer solutions of pH = 4.00 and 7.00 from Metrohm were used to calibrate the pH meter (Metrohm 827 with a Unitrode Pt 1000 combined pH and temperature sensor). The pH values are reported as read from the instrument (after being calibrated to these buffers). MilliQ grade water (ρ = 18.2 MΩ cm, Millipore Direct–Q 3 UV instrument) was used to prepare all solutions.

2.2. Methods

All cyclic voltammetry and galvanostatic electrodeposition experiments were performed using an Autolab 302 type instrument, in a classical 3 electrode electrochemical cell, in which a Pt cage served as the counter electrode, while a Ag/AgCl/sat. KCl electrode (E = +197 mV vs. the standard hydrogen electrode (SHE)) was used as reference. A d = 5 mm Pt disk electrode was used as the working electrode, which was polished on 1 μm sized alumina powder (Buehler) prior to each experiment. The polishing material residues were removed by ultrasonic treatment of the electrode in deionized water. The rotation rate was set to ω = 3000 rpm using an Amatek 636A type instrument during the rotating disk electrode (RDE) experiments.

The electrochemical quartz crystal microbalance (EQCM)

measurements were performed on gold coated quartz crystal electrodes with an oscillatory frequency of 6 MHz. The mass change of the electrode was calculated from the frequency change (Δf), using the Sauerbrey equation (equation (1)):

$$\Delta f = -C_f \times \Delta m \quad (1)$$

The experimental constant was found to be $C_f = 0.0805$ Hz cm^2 ng^{-1} from the calibration experiments (Fig. S1).

The current efficiency measurements were performed in a custom-designed, undivided electrochemical cell using a Hiden HPR-20 mass spectrometer to analyze the cell off-gas. As working electrode, a Pt plate (A = 1 cm^2 for the measurements presented in Fig. 1B, while A = 0.9 cm^2 for those shown in Fig. 3D) was used, while another Pt plate served as counter electrode. The details of the experimental setup were given elsewhere [14]. The HER efficiency was quantified as the ratio of the measured hydrogen production rate (calculated from the flow-rate and the hydrogen content of the cell off-gas) and the maximum H_2 production rate.

2.3. Physical characterization

The Fourier-transform infrared spectroscopy (FT-IR) measurements were performed with a PerkinElmer Spectrum 100 FT-IR type instrument, using a horizontal ATR sampling accessory. The spectra shown in the manuscript were calculated from the average of 32 interferograms. The spectral resolution was set to 1 cm^{-1}. The Raman spectra were recorded using a BWTEK MiniRam type instrument equipped with a λ = 785 nm red laser. The exposure time was set to 10 s, and 10 measurements were averaged. Scanning electron microscopy (SEM) images were collected using a Hitachi S-4800 type instrument at 20 kV accelerating voltage.

The concentration of hypochlorite in the solution was followed with UV–vis spectroscopy, using an Expedeon VersaWave type instrument. V = 200 μl liquid samples were taken by an automatic pipette and were added to 1 cm^3 of 0.5 mol dm^{-3} NaOH. Subsequently the solutions were filled with deionized water to V = 5 cm^3. The UV–vis spectra were recorded using a quartz cuvette (l = 1.000 cm), and the concentration of the hypochlorite was calculated from the absorbance maximum at λ = 292 nm.

3. Results and discussion

3.1. The effect of cerium(III) salt addition on the electrochemical reduction of hypochlorite

In situ induced electrochemical selectivity towards hydrogen evolution reaction (HER) offers the most convenient way to avoid losses due to parasitic cathodic reactions in undivided electrochemical cells. In this case the compound (precursor) which is responsible for the selectivity remains in solution, continuously protecting the surface – just as the chromium (VI) additive in the chlorate synthesis process [1].

The effect of cerium (III) addition was studied in the electrochemical reduction of hypochlorite (Fig. 1). During the cyclic voltammetry (CV) measurements in hypochlorite solution without Ce(III) addition (Fig. 1A) two current plateaus were observed using the Pt RDE. These are related to the diffusion limited reduction of hypochlorous acid and hypochlorite ions, followed by the onset of HER at more negative potentials (linear cathodic current increase below E ≈ −1.25 V). Adding 1 mM $CeCl_3$ to the solution led to the disappearance of the current plateaus, indicating the suppression of electrochemical hypochlorite reduction. On the other hand, the slope of the curve in the HER region was not affected negatively, and the onset potential shifted to less negative values (E ≈ −1.01 V).

After the CV measurements a deposit was observed on the electrode surface. This is likely attributed to the precipitation of cerium hydroxide due to the increased pH on the electrode surface under cathodic polarization [26]. Transferring this electrode to a fresh hypochlorite solution without $CeCl_3$ content, a suppressed hypochlorite reduction was observed (Fig. S2), similar as in the case of the $CeCl_3$ containing solution (Fig. 1A). This clearly shows that the HER selectivity is related to the deposited layer and not to the presence of Ce(III) in the solution.

A significant increase in H_2 production rate was measured upon the cerium salt addition during mass spectrometry coupled galvanostatic experiments performed in a hypochlorite solution (Fig. 1B). Translating these to HER selectivity values (Table 1), an increase from 67% HER efficiency to above 89% was observed after the addition of 1 mM $CeCl_3$ at the highest applied, industrially relevant current density (j = −300 mA cm^{-2}). Note that the increase in HER

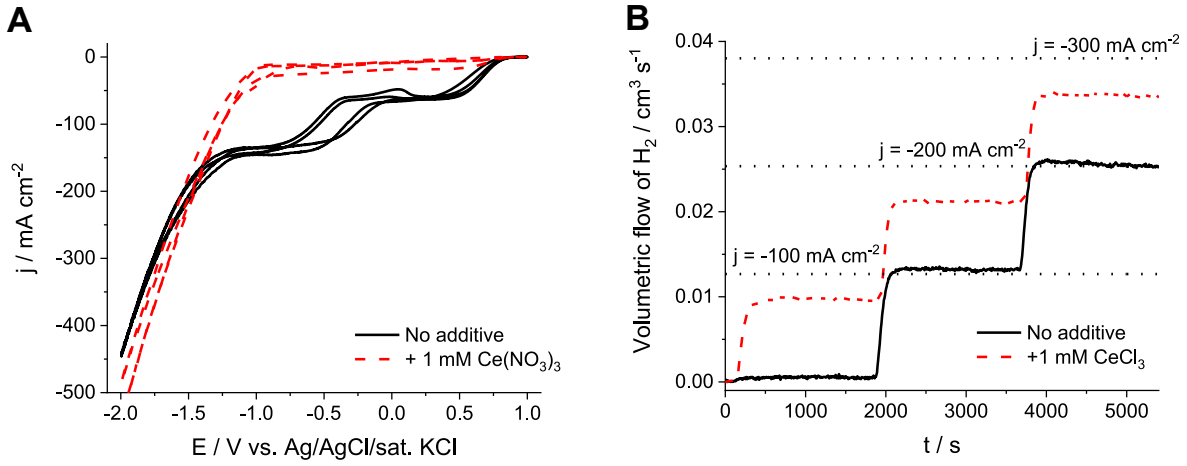

Fig. 1. (A) Cyclic voltammograms recorded using a Pt RDE (ω = 3000 rpm, ν = 10 mV s^{-1}), (B) galvanostatic measurements on a Pt plate electrode (A = 1 cm^2) with mass spectrometric cell off-gas analysis. Both measurements were performed at room temperature in a pH = 6.5 80 mM NaClO +2 M NaCl solution with and without the addition of 1 mM Ce(III) salt to the electrolyte. The dotted horizontal lines in (B) represent the maximum theoretical H_2 production rate at the respective current densities.

Table 1
HER efficiency during a galvanostatic measurement on a bare Pt and a CeO_x coated Pt electrode, calculated from the results shown in Fig. 1B.

|Current density| / mA cm^{-2}	HER efficiency/%		
	100	200	300
Pt	5	52	67
CeO_x/Pt	78	84	89

efficiency after the addition is even more pronounced at lower current densities. The reason behind this is that the partial current density for hypochlorite reduction is limited by mass transport, even in the well-stirred solution, which is not affected by the applied current density. This translates to a higher Faradaic efficiency loss at low overall current densities.

During the galvanostatic measurement, the volumetric flowrate of oxygen was also monitored. This oxygen mainly comes from hypochlorite decomposition on the anode and in the solution bulk [27]. When adding $CeCl_3$ to the hypochlorite solution the oxygen formation rate increases (Fig. S3). Hence, even though the HER efficiency is greatly enhanced by the presence of $CeCl_3$ in the solution, it increases the efficiency losses, related to the unwanted formation of oxygen. Furthermore, at elevated temperatures the evolution of oxygen might also be a safety issue in an undivided electrochemical cell, as an explosive mixture can form (H_2 gas mixtures with above 6 V/V% O_2 can be ignited).

Further, during the galvanostatic measurement the solution gradually turned more turbid due to the precipitation of cerium hydroxide. This is a major drawback of Ce(III) salts as solution additives, especially when compared to the currently used Cr(VI); in this latter case whenever the deposited Cr(III) oxide/hydroxide layer is damaged, or detached from the surface, it is readily oxidized to soluble Cr(VI) species in the electrolyte. Because of the limited solubility of the formed Ce-hydroxide in the bulk electrolyte under operating conditions, depositing CeO_x layers ex situ (rather than forming in situ) is a more realistic option to induce selective HER.

3.2. Electrodeposition of CeO_x layers

CeO_x layers were deposited on the cathode galvanostatically. During this, $Ce(OH)_3$ precipitates on the electrode due to the increased surface pH induced by a cathode reaction (e.g. HER, $2H_2O + 2e^- \rightarrow 2\boldsymbol{OH}^- + H_2$), and is subsequently oxidized by dissolved O_2 in the solution (or by hypochlorite, as discussed below) to Ce(IV) oxide/hydroxide (according to its Pourbaix-diagram) [25]. Monitoring the electrode mass changes during the electroprecipitation at different deposition current densities, a slow mass increase was observed at the beginning of the experiments (Fig. 2). This initial transition is likely attributed to the build-up of high enough hydroxide concentration in the close vicinity of the electrode to precipitate $Ce(OH)_3$. Note that the length of this initial period becomes shorter with increasing current density, which supports this hypothesis. After this initial period the mass increase becomes faster, and the layer grows steadily. This points out that the amount of the electrodeposited material can be effectively controlled by the deposition time [28]. Indeed, the layer growth rate increases with the applied current density, in correlation with the increased hydroxide production rate on the electrode.

Immediately after the deposition, the layers were oxidized by immersing them in alkaline (pH ≈ 13), 500 mM NaOCl solution for 5 min [25]. As our preliminary experiments (not presented here) showed, this step greatly enhanced the adhesion of the layers; the effect of this treatment on the structure and morphology of the electrodes is discussed in chapter 3.3.

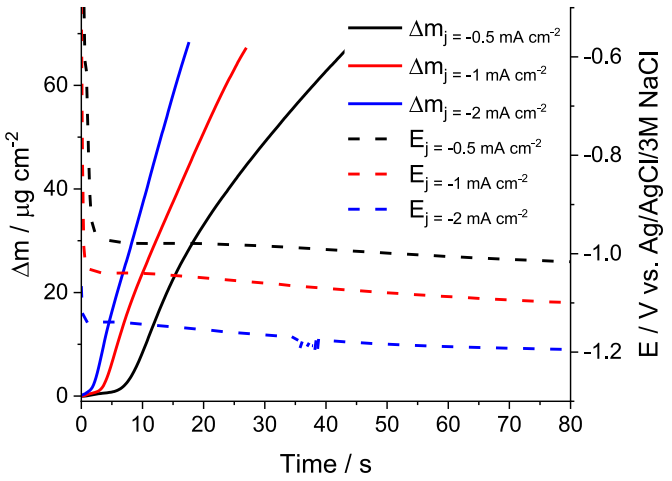

Fig. 2. The change of electrode potential and mass during galvanostatic electrochemical deposition on a Pt EQCM electrode, using 0.025 M $Ce(NO_3)_3$ solution at different current densities.

3.2.1. Optimizing the electrodeposition conditions for hindering the electrochemical reduction of hypochlorite

Layers deposited at varying conditions were first tested in an alkaline solution for the electrochemical reduction of hypochlorite, in which hypochlorite is exclusively present in its deprotonated form. To compare the different coatings, the decrease in the cathodic plateau current (read at E = −1.0 V vs. Ag/AgCl/sat. KCl) served as the figure of merit. To optimize the electrodeposition conditions, the concentration of $Ce(NO_3)_3$, the deposition current density and charge density (deposition time) (Figure S4A, B and C, respectively) were systematically varied. The ratio of the reduction current at E = −1.0 V, measured on the coated electrodes and on the bare Pt electrode was used to describe the efficiency of the coatings, as demonstrated for the case of the effect of the $Ce(NO_3)_3$ concentration in the deposition solution (Fig. 3A).

From the observed results, some general conclusions were drawn: (i) at low $Ce(NO_3)_3$ concentration (1–10 mM) a large cathodic current density (>j = −3 mA cm^{-2}) is needed to deposit the layers, but due to the intense hydrogen bubble evolution the coatings are very inhomogeneous in this case, (ii) at high $Ce(NO_3)_3$ concentration a layer can be deposited even at low cathodic current density (<j = −0.5 mA cm^{-2}), but the adherence of the layers is very poor, these detached easily during the subsequent experiments, (iii) the best layers, in terms of both mechanical stability (adherence) and suppression of electrochemical hypochlorite reduction, are formed at intermediate current densities (j = −1-3 mA cm^{-2}), (iv) the hypochlorite reduction hindering efficiency (as derived from cyclic voltammetry measurements in hypochlorite solutions with the deposited layers) scales with the deposition time (layer thickness), but very long depositions lead to mechanically unstable coatings.

The layers deposited under the optimized conditions (25 mM $Ce(NO_3)_3$ solution, j = −2 mA cm^{-2}, t = 300 s) showed high mechanical and (electro)chemical stability and a greatly suppressed hypochlorite reduction during repetitive cyclic voltammetry measurements; compared to the Pt electrode, a ca. 90% decrease in the hypochlorite reduction current was observed (Fig. 3B). This is also reflected in the recorded polarization curves (Fig. 3C), where both a reduced diffusion limited hypochlorite reduction current (two "sudden potential drops"), and a less negative onset potential for HER (linear range at high current densities) can be observed.

To better quantify the effect of the CeO_x coating on the selectivity towards HER, similar galvanostatic measurements as those in

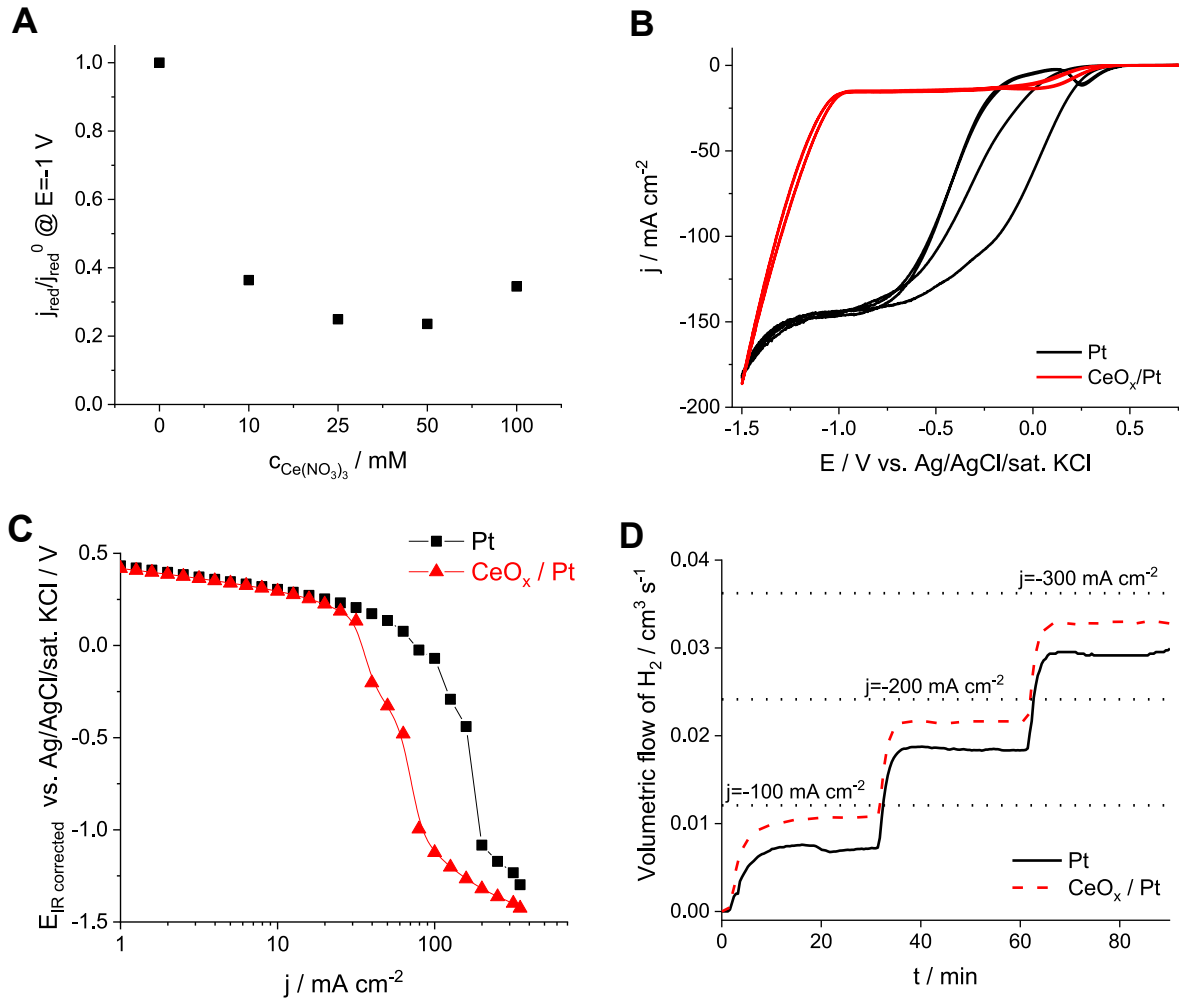

Fig. 3. (A) The ratio of the hypochlorite reduction current at E = −1 V (derived from the measurements shown in (Fig. S4A) on a bare and on CeO_x coated electrodes (deposited for t = 100 s at j = −2 mA cm^{-2} from solutions of different $Ce(NO_3)_3$ concentration). (B) Cyclic voltammograms and (C) polarization curves recorded using bare and CeO_x coated Pt RDEs (ω = 3000 RPM, ν = 10 mV s^{-1}) on which the layers were deposited galvanostatically from a 25 mM $Ce(NO_3)_3$ solution at j = −2 mA cm^{-2} for t = 300 s. The experimental datapoints are only connected by solid lines to guide the eye. (D) Galvanostatic measurements on bare and a CeO_x coated Pt plate electrodes with mass spectrometric cell off-gas analysis. All the measurements were performed at room temperature in a 2 M NaCl containing 80 mM NaClO solution at pH ≈ 12.

Fig. 1B were performed, but without the addition of any cerium salt in the solution (Fig. 3D). In this case as well, the H_2 production rate, which translates to HER efficiency, was significantly higher with the CeO_x coated electrodes as compared to a bare Pt electrode (Table 2). This is further confirmed by the analysis of the hypochlorite concentration during the electrolysis, where a larger hypochlorite concentration increase was found for the coated electrodes (Table S1). On the other hand, the oxygen formation rate (either on the anode electrochemically, or in the solution bulk from the decomposition of hypochlorite) is not affected by the presence of the CeO_x cathode coating (Fig. S5). This clearly shows that a CeO_x layer may potentially act as a protective coating for cathodes used in the chlorate process.

Table 2
HER efficiency during a galvanostatic measurement on a bare Pt and a CeO_x coated Pt electrode, read from Fig. 3D.

|Current density| / mA cm^{-2}	HER efficiency/%		
	100	200	300
Pt	59	76	81
CeO_x/Pt	90	90	91

3.3. Morphology and composition of the deposited layers

In agreement with earlier literature reports, the appearance of the Ce—O symmetric vibration peak at 453 cm^{-1}, and peaks associated with vibrations of residual nitrate ions at 1049 and 742 cm^{-1} are observed on the Raman spectrum of the electrodeposited CeO_x samples that were not exposed to hypochlorite treatment, but were left to be oxidized on air (Fig. 4A), indicating the formation of Ce(IV) oxide [29]. In the case of hypochlorite oxidized samples, the shift of the Ce—O vibration to lower energies (415 cm^{-1}) and the absence of the peak related to the nitrate ions is witnessed. On the other hand, a new peak appearing at 832 cm^{-1} confirms the presence of O—Cl moieties in the layers [29].

The FT-IR spectrum of the electrodeposited, air oxidized samples confirms the presence of nitrate ions (814 and 1314 cm^{-1}) and water in the layers (1640 cm^{-1}, broad peak around 3500 cm^{-1})

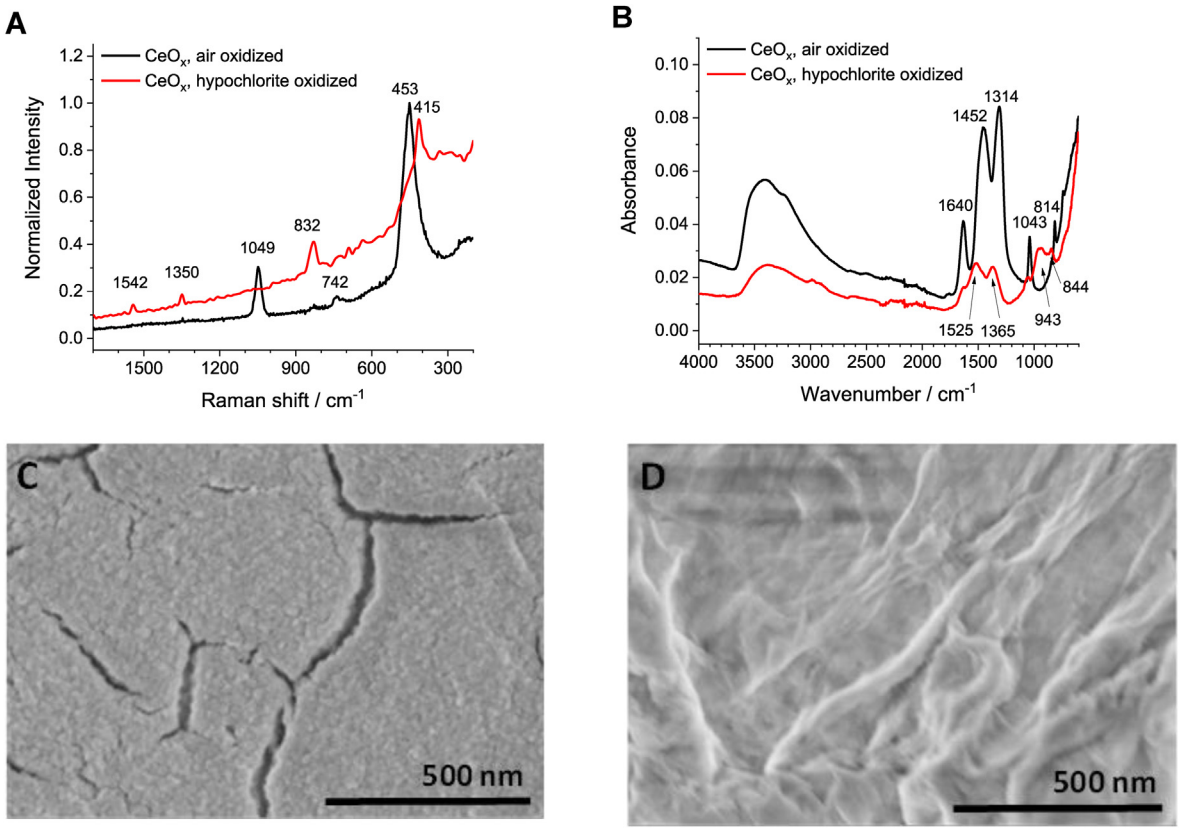

Fig. 4. (A) Raman and (B) FTIR spectra of CeO_x layers electrodeposited for t = 100 s at j = −2 mA cm^{-2} from 25 mM $Ce(NO_3)_3$ solution, oxidized by air exposure or by immersing it in alkaline hypochlorite solution. Typical SEM images of (C) air oxidized and (D) hypochlorite oxidized samples, deposited following the same procedure as in as in (A) and (B).

(Fig. 4B). In the case of the hypochlorite oxidized sample the peaks related to the nitrate ions can no longer be clearly identified. Most importantly, in this case a new peak is seen at 844 cm^{-1} which can be attributed to the stretching vibration of the O–Cl bond [30].

For the air oxidized samples, the layer is formed by the aggregation of <50 nm large particles (Fig. 4C). Some cracks can be observed on the surface, probably formed during drying of the samples. On the other hand, the morphology of the hypochlorite oxidized samples is surprisingly dissimilar from this structure; a coherent film with rough morphology can be seen in which it is difficult to distinguish individual particles (Fig. 4D). Further, the layer is less cracked, which is also observed at lower magnifications (Fig. S6). These measurements highlight that the hypochlorite treatment affects both the chemical composition and the morphology of the deposited layers, leading to mechanically more stable layers.

3.4. Other (reduction) reactions on CeO_x coated electrodes

Similar to the electrochemical reduction of hypochlorite, other mass transport limited electrode reactions, namely the reduction of hydrogen peroxide (Fig. 5A) and dissolved oxygen (Fig. 5B) were investigated using the CeO_x coated electrodes. For both reactions a reduction current plateau was observed on the bare Pt electrode (used as reference), followed by the onset of HER at more negative potentials. As for the CeO_x coated electrodes the current plateau is hardly visible, the currents read in this region are less than 10% of the value for the Pt electrode, whereas the slope of the HER region is not affected negatively; on the contrary, it seems to be even slightly higher.

In the case of H_2O_2 (Fig. 5A), the hindering of the oxidation reaction can be also observed. The oxygen evolution reaction on the other hand proceeds on the modified electrode surface, indicated by the current increase from E ≈ +0.75 V, in accordance with earlier findings on increased anode selectivity towards water oxidation on CeO_x coated electrodes [31].

4. Conclusions

Cerium oxide/hydroxide layers are effective protective layers suppressing the electrochemical reduction of hypochlorite. The kinetics of the electrochemical hydrogen evolution is not affected significantly by the coating. Adding cerium (III) precursor to a hypochlorite solution, such a protective coating can be formed in situ during chlorate electrolysis. The precipitation of the precursor in the form of cerium hydroxide in the electrolyte bulk, the mechanical instability of these coatings and the increased oxygen formation are however major drawbacks using this approach. Mechanically and chemically (even when exposed to hypochlorite solution without any cathodic protection) stable cerium oxide layers can be formed ex situ by electrodeposition on electrodes under carefully optimized conditions. Using these CeO_x coated electrodes, a significant selectivity increase towards HER in hypochlorite containing solutions was achieved, even at high, industrially relevant current densities. Cerium oxide based materials are therefore promising candidates as protective layers on cathodes used in the industrial electrolytic production of sodium chlorate. Aiming this, the long-term chemical and mechanical stability, and the ability of these layers to protect the underlaying substrate from corrosion by hypochlorite needs to be addressed first under laboratory conditions, and subsequently in pilot plants.

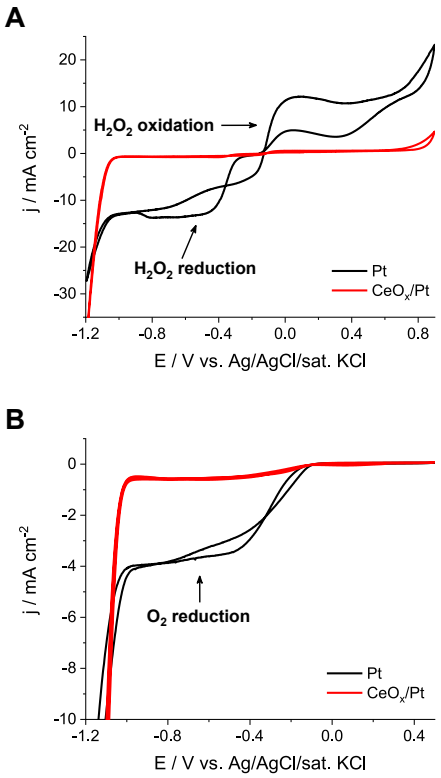

Fig. 5. Cyclic voltammograms recorded on bare Pt and electrodeposited CeO_x coated Pt (t = 300 s at j = −2 mA cm^{-2} from 25 mM $Ce(NO_3)_3$) RDEs (ω = 3000 rpm, ν = 10 mV s^{-1}), in 1 M NaOH solution (A) with the addition of 10 mM H_2O_2, N_2 purged, (B) saturated with O_2. The 2nd cycles are shown in both cases.

Declaration of competing interest

The authors declare that they have no known competing financial interests or personal relationships that could have appeared to influence the work reported in this paper.

CRediT authorship contribution statement

Balázs Endrődi: Conceptualization, Investigation, Writing - original draft, Visualization, Formal analysis. **Oscar Diaz-Morales:** Writing - review & editing, Formal analysis, Visualization, Investigation. **Ulriika Mattinen:** Writing - review & editing, Visualization. **Maria Cuartero:** Writing - review & editing, Resources. **Aiswarya Krishnakumar Padinjarethil:** Writing - review & editing, Investigation. **Nina Simic:** Writing - review & editing, Supervision. **Mats Wildlock:** Writing - review & editing, Supervision. **Gaston A. Crespo:** Resources, Supervision. **Ann Cornell:** Conceptualization, Writing - review & editing, Supervision.

Acknowledgement

The financial support from the Swedish Energy Agency and Nouryon Pulp and Performance Chemicals is gratefully acknowledged.

Appendix A. Supplementary data

Supplementary data to this article can be found online at https://doi.org/10.1016/j.electacta.2020.136022.

References

[1] B. Endrődi, N. Simic, M. Wildlock, A. Cornell, A review of chromium(VI) use in chlorate electrolysis: functions, challenges and suggested alternatives, Electrochim. Acta 234 (2017) 108–122, https://doi.org/10.1016/j.electacta.2017.02.150.
[2] B. Endrődi, G. Bencsik, F. Darvas, R. Jones, K. Rajeshwar, C. Janáky, Continuous-flow electroreduction of carbon dioxide, Prog. Energy Combust. Sci. 62 (2017) 133–154, https://doi.org/10.1016/j.pecs.2017.05.005.
[3] P. Millet, R. Ngameni, S.a. Grigoriev, N. Mbemba, F. Brisset, a. Ranjbari, C. Etiévant, PEM water electrolyzers: from electrocatalysis to stack development, Int. J. Hydrogen Energy 35 (2010) 5043–5052, https://doi.org/10.1016/j.ijhydene.2009.09.015.
[4] S. Lakshmanan, T. Murugesan, The chlor-alkali process: work in Progress, Clean Technol. Environ. Policy 16 (2014) 225–234, https://doi.org/10.1007/s10098-013-0630-6.
[5] A. Cornell, Encyclopedia of Applied Electrochemistry, Springer New York, New York, NY, 2014, https://doi.org/10.1007/978-1-4419-6996-5.
[6] T. Hisatomi, K. Takanabe, K. Domen, Photocatalytic water-splitting reaction from catalytic and kinetic perspectives, Catal. Lett. 145 (2015) 95–108, https://doi.org/10.1007/s10562-014-1397-z.
[7] M. Yoshida, K. Takanabe, K. Maeda, A. Ishikawa, J. Kubota, Y. Sakata, Y. Ikezawa, K. Domen, Role and function of noble-metal/Cr-layer core/shell structure cocatalysts for photocatalytic overall water splitting studied by model electrodes, J. Phys. Chem. C 113 (2009) 10151–10157, https://doi.org/10.1021/jp901418u.
[8] K. Maeda, K. Teramura, D. Lu, N. Saito, Y. Inoue, K. Domen, Noble-metal/Cr_2O_3 core/shell nanoparticles as a cocatalyst for photocatalytic overall water splitting, Angew. Chem. Int. Ed. 45 (2006) 7806–7809, https://doi.org/10.1002/anie.200602473.
[9] K. Maeda, K. Teramura, D. Lu, N. Saito, Y. Inoue, K. Domen, Roles of Rh/Cr_2O_3 (Core/Shell) nanoparticles photodeposited on visible-light-responsive ($Ga_{1-x}Zn_x$)($N_{1-x}O_x$) solid solutions in photocatalytic overall water splitting, J. Phys. Chem. C 111 (2007) 7554–7560, https://doi.org/10.1021/jp071056j.
[10] M. Qureshi, T. Shinagawa, N. Tsiapis, K. Takanabe, Exclusive hydrogen generation by electrocatalysts coated with an amorphous chromium-based layer achieving efficient overall water splitting, ACS Sustain. Chem. Eng. 5 (2017) 8079–8088, https://doi.org/10.1021/acssuschemeng.7b01704.
[11] D. V Esposito, Membrane-coated electrocatalysts—an alternative approach to achieving stable and tunable electrocatalysis, ACS Catal. 8 (2018) 457–465, https://doi.org/10.1021/acscatal.7b03374.
[12] J. Gustavsson, L. Nylén, A. Cornell, Rare earth metal salts as potential alternatives to Cr(VI) in the chlorate process, J. Appl. Electrochem. 40 (2010) 1529–1536, https://doi.org/10.1007/s10800-010-0136-4.
[13] M. Li, Z. Twardowski, F. Mok, N. Tam, Sodium molybdate—a possible alternate additive for sodium dichromate in the electrolytic production of sodium chlorate, J. Appl. Electrochem. 37 (2007) 499–504, https://doi.org/10.1007/s10800-006-9281-1.
[14] B. Endrődi, S. Sandin, V. Smulders, N. Simic, M. Wildlock, G. Mul, B.T. Mei, A. Cornell, Towards sustainable chlorate production: the effect of permanganate addition on current efficiency, J. Clean. Prod. 182 (2018) 529–537, https://doi.org/10.1016/j.jclepro.2018.02.071.
[15] B. Endrődi, V. Smulders, N. Simic, M. Wildlock, G. Mul, B. Mei, A. Cornell, In situ formed vanadium-oxide cathode coatings for selective hydrogen production, Appl. Catal. B Environ. 244 (2019) 233–239, https://doi.org/10.1016/j.apcatb.2018.11.038.
[16] A.S.O. Gomes, M. Busch, M. Wildlock, N. Simic, E. Ahlberg, Understanding selectivity in the chlorate process: a step towards efficient hydrogen production, Chemistry 3 (2018) 6683–6690, https://doi.org/10.1002/slct.201800628.
[17] K. Hedenstedt, A.S.O. Gomes, M. Busch, E. Ahlberg, Study of hypochlorite reduction related to the sodium chlorate process, Electrocatalysis 7 (2016) 326–335, https://doi.org/10.1007/s12678-016-0310-5.
[18] G. Lindbergh, D. Simonsson, The effect of chromate addition on cathodic reduction of hypochlorite in hydroxide and chlorate solutions, J. Electrochem. Soc. 137 (1990) 3094, https://doi.org/10.1149/1.2086165.
[19] B. Endrődi, S. Sandin, M. Wildlock, N. Simic, A. Cornell, Suppressed oxygen evolution during chlorate formation from hypochlorite in the presence of chromium(VI), J. Chem. Technol. Biotechnol. 94 (2019) 1520–1527, https://doi.org/10.1002/jctb.5911.
[20] J. Wanngård, M. Wildlock, The catalyzing effect of chromate in the chlorate formation reaction, Chem. Eng. Res. Des. 121 (2017) 438–447, https://doi.org/10.1016/j.cherd.2017.03.021.
[21] J. Kalmár, M. Szabó, N. Simic, I. Fábián, Kinetics and mechanism of the chromium(VI) catalyzed decomposition of hypochlorous acid at elevated temperature and high ionic strength, Dalton Trans. 47 (2018) 3831–3840, https://doi.org/10.1039/C8DT00120K.
[22] B. Endrődi, A. Stojanovic, M. Cuartero, N. Simic, M. Wildlock, R. de Marco, G.A. Crespo, A. Cornell, Selective hydrogen evolution on manganese oxide coated electrodes: new cathodes for sodium chlorate production, ACS Sustain. Chem. Eng. 7 (2019) 12170–12177, https://doi.org/10.1021/acssuschemeng.9b01279.
[23] A. Gebert, M. Lacroix, O. Savadogo, R. Schulz, Cathodes for chlorate electrolysis with nanocrystalline Ti–Ru–Fe–O catalyst, J. Appl. Electrochem. 30 (2000)

1061–1067, https://doi.org/10.1023/A:1004030706423.
[24] L. Gajic-Krstajic, N. Elezovic, B. Jovic, G. Martelli, V. Jovic, N. Krstajic, Fe-Mo alloy coatings as cathodes in chlorate production process, Hem. Ind. 70 (2016) 81–89, https://doi.org/10.2298/HEMIND150119014G.
[25] M. Pourbaix, Atlas of Electrochemical Equilibria in Aqueous Solutions, National Association of Corrosion Engineers, 1974. https://books.google.hu/books?id=QjxRAAAAMAAJ.
[26] X. Wang, F. Fan, J.A. Szpunar, Optimizing cathodic electrodeposition parameters of ceria coating to enhance the oxidation resistance of a Cr_2O_3-forming alloy, Thin Solid Films 611 (2016) 12–20, https://doi.org/10.1016/j.tsf.2016.05.004.
[27] R.K.B. Karlsson, A. Cornell, Selectivity between oxygen and chlorine evolution in the chlor-alkali and chlorate processes, Chem. Rev. 116 (2016) 2982–3028, https://doi.org/10.1021/acs.chemrev.5b00389.
[28] L. Yang, X. Pang, G. Fox-Rabinovich, S. Veldhuis, I. Zhitomirsky, Electrodeposition of cerium oxide films and composites, Surf. Coating. Technol. 206 (2011) 1–7, https://doi.org/10.1016/j.surfcoat.2011.06.029.
[29] K. Nakamoto, Infrared and Raman Spectra of Inorganic and Coordination Compounds, John Wiley & Sons, Inc., Hoboken, NJ, USA, 2008, https://doi.org/10.1002/9780470405840.
[30] A. Draksharapu, D. Angelone, M.G. Quesne, S.K. Padamati, L. Gómez, R. Hage, M. Costas, W.R. Browne, S.P. de Visser, Identification and spectroscopic characterization of nonheme iron(III) hypochlorite intermediates, Angew. Chem. 127 (2015) 4431–4435, https://doi.org/10.1002/ange.201411995.
[31] K. Obata, K. Takanabe, A permselective CeO_x coating to improve the stability of oxygen evolution electrocatalysts, Angew. Chem. Int. Ed. 57 (2018) 1616–1620, https://doi.org/10.1002/anie.201712121.